

Where are Mars' Hypothesized Ocean Shorelines? Large Lateral and Topographic Offsets Between Different Versions of Paleoshoreline Maps.

Steven F. Sholes^{1,2}, Zachary I. Dickeson^{3,4}, David R. Montgomery¹, and David C. Catling^{1,2}

¹Department of Earth and Space Sciences, University of Washington, Seattle, WA, USA.

²Astrobiology Program, University of Washington, Seattle, WA, USA.

³Department of Earth Sciences, Natural History Museum, London, UK.

⁴Department of Earth and Planetary Sciences, Birkbeck College, University of London, London, UK.

Corresponding author: Steven F. Sholes (sfsholes@uw.edu)

Key Points:

- Remapping segments of the putative Mars shorelines finds modern maps diverge by up to 500 km from their original geomorphic descriptions.
- Variance of published global putative shorelines is large: for the Arabia Level, a mean lateral offset of 360 km with 1,350 km peak offset.
- The large topographic disparity of the Arabia Level can be explained through these inconsistent mappings over time.

1 **Abstract**

2 Mars' controversial hypothesized ocean shorelines have been found to deviate significantly from
3 an expected equipotential surface. While multiple different deformation models have been
4 proposed to explain the wide range of elevations, here we show that the historical locations used
5 in the literature and in these models varies widely. We find that the most commonly used version
6 of the Arabia Level does not follow the originally described contact and can deviate laterally by
7 ~500 km in Deuteronilus Mensae. A meta-analysis of the different shapefiles used for the Arabia
8 Level shows that, globally, the location of putative shoreline varies by an average of 360 km and
9 up to 1350 km along the topographic dichotomy. This leads to mean elevations of the level that
10 vary by up to 1.7 km between different shapefiles, and topographic ranges within each shapefile
11 ranging from 3.0 to 8.7 km. The younger Deuteronilus Level has less variation as it largely
12 follows a formal contact (the Vastitas Borealis Formation) within the relatively flat northern
13 plains. Given the high variance in position (spatial and topographic) of the levels, the use of such
14 shapefiles and conclusions based on them are potentially problematic.

15 **Plain Language Summary**

16 Whether oceans ever existed on Mars is controversial, with support largely coming from
17 hypothesized ancient shorelines. As with modern Earth shorelines, these possible ancient martian
18 ones are expected to be approximately level, but past studies found that the two main global
19 shoreline mappings have elevation ranges from about one to several kilometers, respectively.
20 Here, we remap segments of the proposed shorelines based on their original geomorphic
21 definitions and find that modern maps vary laterally by hundreds of kilometers from our more
22 accurate placements. Additionally, we compare maps of potential shorelines over time. We find
23 that maps are both inconsistent and inaccurate with their placement of hypothesized shorelines.
24 Lateral offsets between different maps exceed a thousand kilometers. This disagreement with the
25 poorly-understood location of the potential shorelines can explain, in part, the observed elevation
26 differences. Our results suggest the limited usefulness of putative shorelines as evidence for
27 ancient martian oceans and the need for more detailed, revised mappings and scrutiny.

28 **1 Introduction**

29 Multiple ocean shorelines have been proposed that encircle the northern plains of Mars
30 but they are controversial (e.g., Carr & Head, 2003). Past oceans would imply many constraints
31 on the past climate, habitability, and hydrological evolution of the planet. Putative
32 paleoshorelines have been described as “the most compelling evidence that Mars once had
33 oceans” (Zuber, 2018), but two major problems confront their interpretation: 1) detailed
34 localized geomorphological studies of the putative shorelines consistently find little to no
35 evidence of coastal landforms (e.g., Ghatan & Zimbelman, 2006; Malin & Edgett, 1999; Sholes
36 et al., 2019) contrary to broader regional analyses (e.g., Clifford & Parker, 2001; Parker et al.,
37 1993; Parker et al., 2010; Parker et al., 1989), and 2) the mapped features vary by multiple
38 kilometers in elevation across the planet in contrast to an expected equipotential surface (Carr &
39 Head, 2003) (Figure 1). Here, we set aside the controversial validity of these features as
40 paleoshorelines and, rather, address the mapped locations of the features and how that affects
41 their topographic expression and, by extension, their interpretation.

42 There are two primary proposed paleoshoreline features, which we hereafter refer to with
43 the non-genetic term “levels,” following Parker et al. (2010). These two levels have been

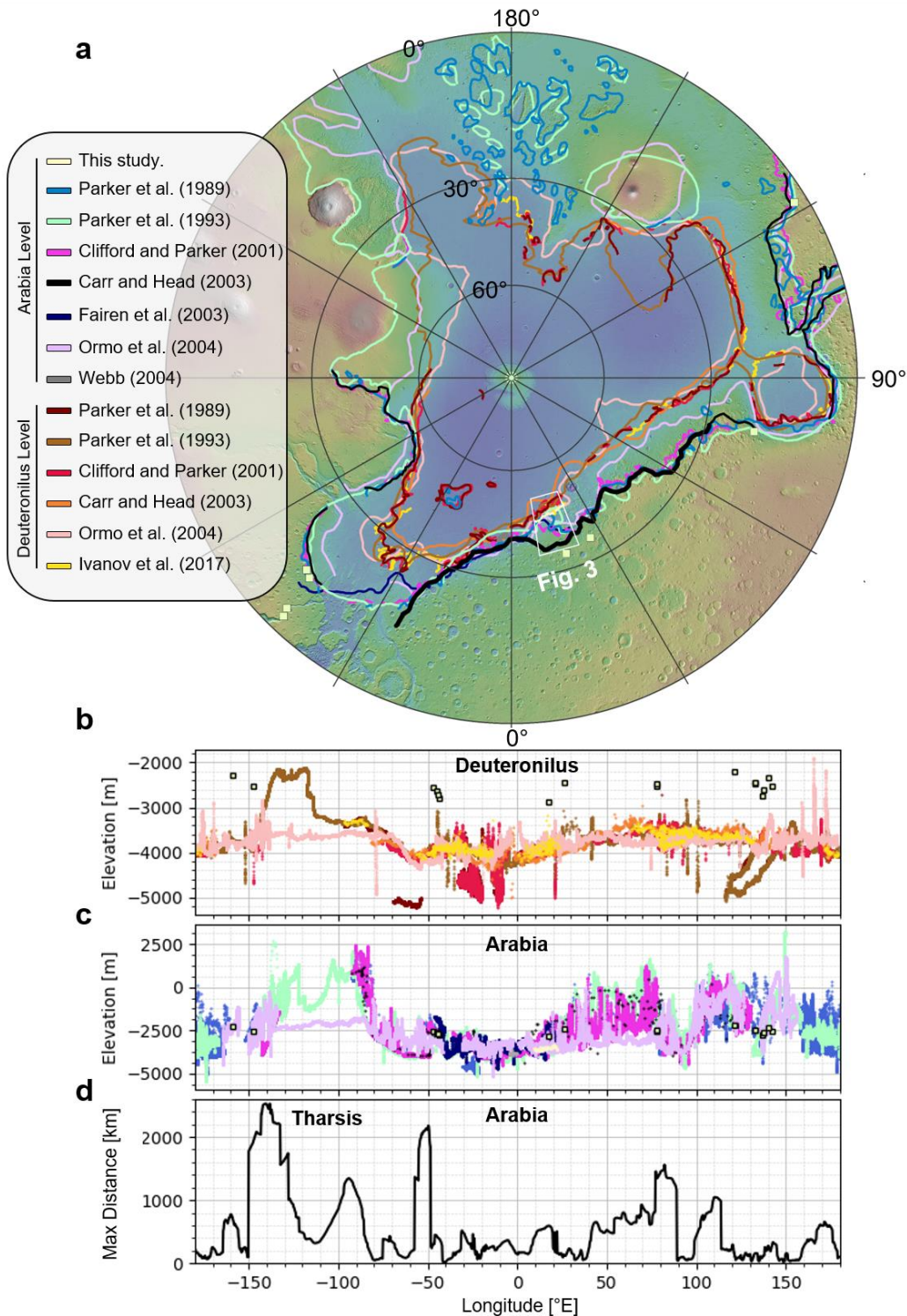


Figure 1: Locations of putative martian shorelines. *a*) Polar projection showing the composite locations of the Arabia and Deuteronilus Levels as found in various published figures. The bold black line indicates the Arabia Level segment from Carr and Head (2003) used in deformation models (e.g., Perron et al. (2007), Citron et al. (2018), Chan et al. (2018)). Yellow squares are the open deltas from di Achille and Hynes (2010). *b* and *c*) Topography of the Deuteronilus and Arabia Levels respectively, with open deltas shown as yellow squares. *d*) The maximum longitudinal distance between all versions of the Arabia Level along each longitude showing 10^2 - 10^3 km discrepancies.

45 mapped to near-complete closure around the northern plains: 1) the Arabia Level (“Contact 1” in
46 the early literature) that roughly follows the topographic dichotomy and has been hypothesized
47 to represent a large early ocean stand; and 2) the Deuteronilus Level (“Contact 2” in the early
48 literature) which largely follows the southern boundary of the Hesperian-aged Vastitas Borealis
49 Formation (VBF) in the northern plains (Tanaka et al., 2005). Various other levels have been
50 mapped, e.g., the Ismenius, Acidalia, and Meridiani Levels (Edgett & Parker, 1997; Parker et al.,
51 2010), but these are not as thoroughly studied or mapped globally.

52 While interpretations of these two main hypothesized levels were originally based on a
53 few high-resolution Viking images (~10 m/px) along Mamers Valles, global maps were created
54 predominantly using low-resolution Viking data (>100 m/px) (Parker et al., 1993; Parker et al.,
55 1989). An updated map for both levels was included in Clifford and Parker (2001), which took
56 advantage of a few higher-resolution Mars Orbiter Camera (MOC) (Malin & Edgett, 2001)
57 imagery. However, since then, little work has been published to provide updated global maps of
58 the Arabia Level using now-available high-resolution data, e.g., nearly-global Context Camera,
59 CTX with coverage at 6-10 m/px (Malin et al., 2007). A small segment of the Arabia Level was
60 remapped by Webb (2004) to circumvent the Bamberg Crater ejecta blanket, but this appears to
61 be largely based on maintaining a mean elevation rather than on observed geomorphology. In
62 contrast, the Deuteronilus Level has been updated in a global map by Ivanov et al. (2017) using
63 Thermal Emission Imaging System (THEMIS) infrared daytime mosaics at ~100 m/px
64 (Christensen et al., 2004).

65 Absolute elevations of the levels were first analyzed in detail by Head et al. (1999);
66 (1998) with limited Mars Orbiter Laster Altimeter (MOLA) data (Smith et al., 2001), which was
67 later expanded on by Carr and Head (2003). The Deuteronilus Level was found to approximate
68 an equipotential surface with a mean elevation of -3.79 ± 0.24 km. While the standard deviation
69 was relatively small, it was not negligible and a total elevation range of 1.2 km was mapped,
70 casting doubt on a paleoequipotential surface. The Arabia Level was found to have a mean
71 elevation of -2.09 ± 1.4 km. With such a large standard deviation and total range of 5.85 km, the
72 authors all-but-dismissed the Arabia Level as a possible paleoshoreline and mass wasting or
73 volcanism were suggested as mechanisms for producing the mapped boundary.

74 Remapping of the Detueronilus Level by Ivanov et al. (2017) gave an updated mean
75 elevation of -3.76 ± 0.21 km (interdecile range of -4.02 to -3.48 km). However, the authors found
76 that the data was better fit by two distinct regional topographic levels with one area
77 encompassing the Tempe, Chryse, Acidalia, and Cydonia-Deuteronilus regions, having a mean
78 elevation of -3.92 km (interdecile range of -4.01 to -3.83 km), along with the area composed of
79 the Pyramus-Astapus, Utopia, and Western Elysium regions, having a mean elevation of -3.58
80 km (interdecile range of -3.73 to -3.46 km).

81 Multiple physical processes have been hypothesized to explain these drastic
82 discrepancies in elevations. Early models invoked isostatic rebound caused by the dissipation of
83 the water (Leverington & Ghent, 2004), thermal isostasy (Ruiz et al., 2004), and mantle plumes
84 (Roberts & Zhong, 2004). Later work integrated the mapped levels shapefiles to argue that true
85 polar wander (Ivanov et al., 2017; Perron et al., 2007), crustal flexure (Citron et al., 2018), or a
86 combination of the two processes (Chan et al., 2018) could account for the long-wavelength
87 topographic deformation. However, these models are still unable to fully explain the large spread
88 of elevations along the modeled paleo-topography for the Arabia Level and the results excluded
89 vast sections of the mapped level, only testing against the level within Arabia Terra.

90 Many of the mapped levels currently in use (primarily the Arabia Level and the pre-
91 Ivanov et al. (2017) Deuteronilus Level) stem from shapefiles created by Carr and Head (2003)
92 which, in turn, were datamined from the map in Clifford and Parker (2001). This has introduced
93 additional errors as to the exact location of the levels originally identified by Parker et al. and
94 may contribute a substantial portion of the large topographic ranges observed. Problems
95 associated with map projections, line thicknesses, figure resolutions, and sampling points are
96 compounded with the already uncertain position of the levels. Clifford and Parker (2001) note
97 that the levels were “often at the borderline of detectability” and their attempts to correlate them
98 across the planet “invariably led to some misidentifications.” The Arabia Level was largely
99 mapped as a series of numerous discontinuous local benches which the authors note may be
100 “manifestations of some other phenomena” rather than coastal terraces. Delineating these
101 benches also proved difficult during the digitization in Carr and Head (2003) so a smoothed and
102 extrapolated loose fit of the level was performed, especially in Deuteronilus Mensae.
103 Subsequently, we refer to this loose fit of the level as a “regional generalization”.

104 In particular, the Mamers Valles region was essentially used as a ‘type locality’ for
105 describing the Arabia Level (Parker et al., 1989, their Fig. 4), yet in most maps (primarily those
106 based in part off the Carr and Head (2003) digitization) the level wholly circumvents the Mamers
107 region to the south. This reiterates one of the major underlying problems with the proposed
108 shorelines: whether the observed topographic range is representative of the mapped levels or
109 whether the features are not truly continuous or marine in origin (Carr & Head, 2019). Thus, we
110 quantify variations in how the Arabia and Deuteronilus Levels have been mapped over time and
111 the associated errors that are caused by data handling, digitization of published maps, and low-
112 resolution mapping.

113 **2 Methods/Data**

114 **2.1 Remapping Levels in Deuteronilus Mensae**

115 The Arabia Level is difficult to map because the level exhibits a range of geomorphic
116 expressions along track and is often discontinuous (Parker et al., 2010; Sholes et al., 2019). For
117 mapping, we use the level description provided in Parker et al. (2010): a sharp albedo contact
118 between the dark-toned northern plains material and the light-toned upper highlands material.
119 This albedo contrast can be difficult to distinguish in the full-coverage high-resolution CTX
120 imagery, but is apparent in the THEMIS-IR daytime mosaics, so we use a combination of both.
121 High Resolution Imaging Science Experiment (HiRISE, (McEwen et al., 2007)) data is very
122 sparse and insufficient across the boundary and thus not examined here.

123 Using ArcGIS 10.6 (www.esri.com), we map the albedo contact using layered CTX and
124 THEMIS-IR daytime mosaics across the Deuteronilus Mensae region (see Figure 2). The contact
125 is bounded to the east by the Lyot Crater ejecta blanket and to the west by a distinct differently
126 toned dark lowland unit originally mapped as part of the Arabia Level by Parker et al. (1989).
127 However, more recent detailed studies suggest that this contact is the result of localized pooling
128 from catastrophic overland-flow megafloods with no indication of prior standing water (Mangold
129 & Howard, 2013; Sholes, 2019). Thus, we do not include this unit boundary in our mapping.

130 As we only map the albedo contact where it is distinct and recognizable based on the
131 aforementioned definition, many of the small discontinuous segments included in the

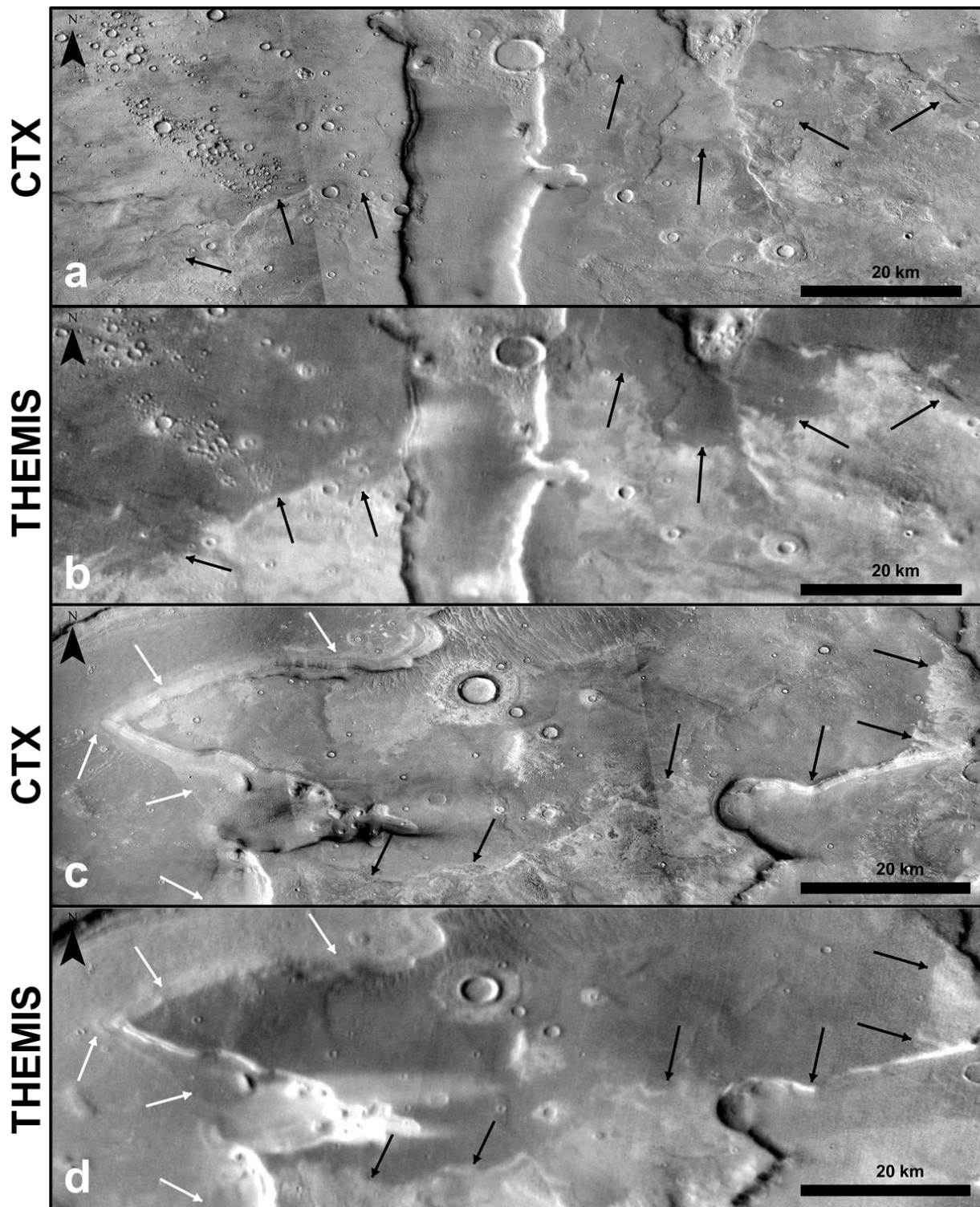


Figure 2: Remapping examples of the Arabia Level within Deuteronilus Mensae. *a)* CTX mosaic of original location used to define the Arabia Level along Mamers Valles. Black arrows indicate location of the contact we map. *b)* THEMIS-IR daytime mosaic of region in *a* showing the distinct albedo contrast used to map the level. *c)* CTX mosaic of a mesa within the dissected terrain that is crosscut by the albedo contact. White arrows indicate the Deuteronilus Level as mapped by Ivanov et al. (2017) and black arrows indicate our mapping of the Arabia Level. *d)* THEMIS-IR daytime mosaic of *c*.

133 Clifford and Parker (2001) map are excluded here. These numerous features are largely proposed
134 small benches and terraces that line the valley walls of the regional dissected terrain, but were
135 noted by the authors to likely be possible manifestations of non-marine processes. These valleys
136 have also been subjected to recent (late Amazonian) glacial modification (e.g., Baker & Head,
137 2015; Morgan et al., 2009). Levels were not interpolated across gaps where they were either not
138 present (e.g., valleys) or eroded/buried.

139 We also remap a small portion of the Deuteronilus Level ~500 km west of Mammers
140 Valles that had previously been identified as potentially deviating from the Ivanov et al. (2017)
141 mapping (Sholes, 2019). As the level was originally mapped primarily with THEMIS-IR, we
142 map using the high-resolution CTX data while following the same procedures and definitions
143 therein. Here, the contact is defined largely by the southward-facing lobate flowfronts rather than
144 a textural or albedo contact.

145 2.2 Global Map Comparisons

146 We also compare different published mappings of the levels to quantify the lateral and
147 topographic variance (Clifford & Parker, 2001; Fairen et al., 2003; Ormö et al., 2004; Parker et
148 al., 1993; Parker et al., 1989; Webb, 2004). Inquiries were made of many researchers in the
149 community about the availability of shapefiles for mapped levels of proposed Mars shorelines
150 (Carr & Head, 2003; Ivanov et al., 2017; Parker et al., 2010; Perron et al., 2007; Webb, 2004).
151 Shapefiles were generously shared by Mikhail Ivanov and Taylor Perron (personal
152 communication). Where shapefiles were not available from the original authors, we digitally
153 traced the levels from the published figures. Each figure image is georeferenced into ArcGIS
154 using the matching projection to ensure a good fit. Figures with no coordinates were
155 georeferenced to major crater centers. A polyline was then manually constructed over the center
156 of each mapped level, with vertices spaced at distances approximate to the line width of the
157 mapped level on the original figure. In this way, the geometry, position, and resolution of each
158 mapped level was replicated in the new shapefiles.

159 As with our remapping of Arabia Level in Deuteronilus Mensae, all elevations are
160 compared using the blended MOLA/HRSC (High Resolution Stereo Camera (Jaumann et al.,
161 2007)) elevation model at 200 m/px (Ferguson et al., 2018). We do not make any generalizations
162 or lateral interpolations of the levels nor do we map the numerous small discontinuous benches
163 such as found in Clifford and Parker (2001).

164 To quantify the lateral variance between the various published versions of each level, we
165 opt to calculate the maximum latitudinal geodesic distance between the northernmost and
166 southernmost shapefiles (disregarding the detached ‘islands’ in the northern plains) at regularly-
167 spaced longitudinal cross-sections (every 0.25°). Due to the nature of the levels being both
168 irregular and mapped on a spheroid, this method only provides a quick, first-order approximation
169 of the lateral variance. It is inadequate for sections that track near-longitudinally (opposed to
170 near-latitudinally), for which comparing the maximum distance between the westernmost and
171 easternmost shapefiles at the same latitude would better characterize the maximum variance.
172 However, the Arabia Level tracks circumpolar, so this method provides a good approximation to
173 its global variance.

174 **3 Results & Discussion**

175 3.1 Remapping within Deuteronilus Mensae

176 We find that the Arabia Level, as mapped using the base definition provided in Parker et
 177 al. (1989) within Deuteronilus Mensae, deviates by up to 500 km from the shapefiles made by
 178 Carr and Head (2003). These shapefiles have ‘traditionally’ been used in various analyses (e.g.,
 179 Chan et al., 2018; Citron et al., 2018; Perron et al., 2007). Figure 3a presents a direct comparison
 180 between our remapped Arabia Level, the Carr and Head (2003) shapefiles, and the updated
 181 Deuteronilus Level shapefile from Ivanov et al. (2017). This offset is largely the result of the
 182 regional generalization of the Arabia Level done by Carr and Head (2003) due to aggregation of
 183 the numerous small discontinuous segments (e.g., putative benches and terraces along the valley
 184 and mesa walls).

185 The large offset between the different Arabia Level versions within Deuteronilus Mensae
 186 corresponds to an average elevation difference of ~ 1.13 km (Figure 3b). Our remapping of the
 187 Arabia Level finds an average elevation of -3.56 ± 0.08 km (with an interdecile range of 200 m),
 188 while the datamined version from Carr and Head (2003) had a local mean elevation of -
 189 2.62 ± 0.47 km (with an interdecile range of 1,180 m). This topographic variability is observed
 190 spatially in Figure 3a where the traditional Arabia Level is positioned further south in the
 191 highlands, crosscuts large craters and valley networks, and has a data resolution of ~ 50 km. This
 192 disparity is further compounded by the fact that the Arabia Level straddles the topographic
 193 dichotomy, so even relatively small offsets can lead to greater amounts of elevation differences.

194 While the Arabia Level exhibits different morphologies (onlapping, gradational, and
 195 terraces) (Parker et al., 2010), here it seems to simply demarcate the early Hesperian transitional
 196 (eHt) and late Noachian highland (INh) units (Tanaka et al., 2014) (Figure A1 in Appendix A).
 197 The exception is where the albedo contact crosses the mesas within the dissected terrain. Here,
 198 the southern boundary of the contact often follows the southern edges of the mesas, which
 199 implies that the mapped segments may only be the current southernmost exposure of these units.
 200 Due to the erosive processes in the region, the current contact may be unrepresentative of the
 201 level’s paleotopography.

202 The Deuteronilus Level, remapped by Ivanov et al. (2017), varies by much less than the
 203 Arabia Level in this region, even when compared to the old datamined versions, with a
 204 topographic offset of ~ 160 m. This is likely due to the relative flatness of the northern plains
 205 (Aharonson et al., 2001; Smith et al., 1998), so even with a maximum lateral offset of ~ 400 km,
 206 the topographic disparity is low.

207 However, despite the detailed, improved maps made by Ivanov et al. (2017) for the
 208 Deuteronilus Level, we find that due to both the resolution of their THEMIS-IR mapping (100
 209 m/px) versus the available CTX data (6-10 m/px) and the variable nature of the VBF that it
 210 follows (described below), there are some sections that are incomplete or offset from the base
 211 definition. Figure 4 shows the segment of the Deuteronilus Level that we remapped ~ 500 km
 212 west of Mavors Valles (Figure 3) where this offset placement is readily discernible. Here, there
 213 are three primary differences in how the level is mapped: *A*) small underlying lobate flows of the
 214 VBF that extend beyond the mapped contact; these are virtually indistinguishable in the
 215 THEMIS-IR mosaics but pronounced in visual imagery; *B*) sections where the contact is too

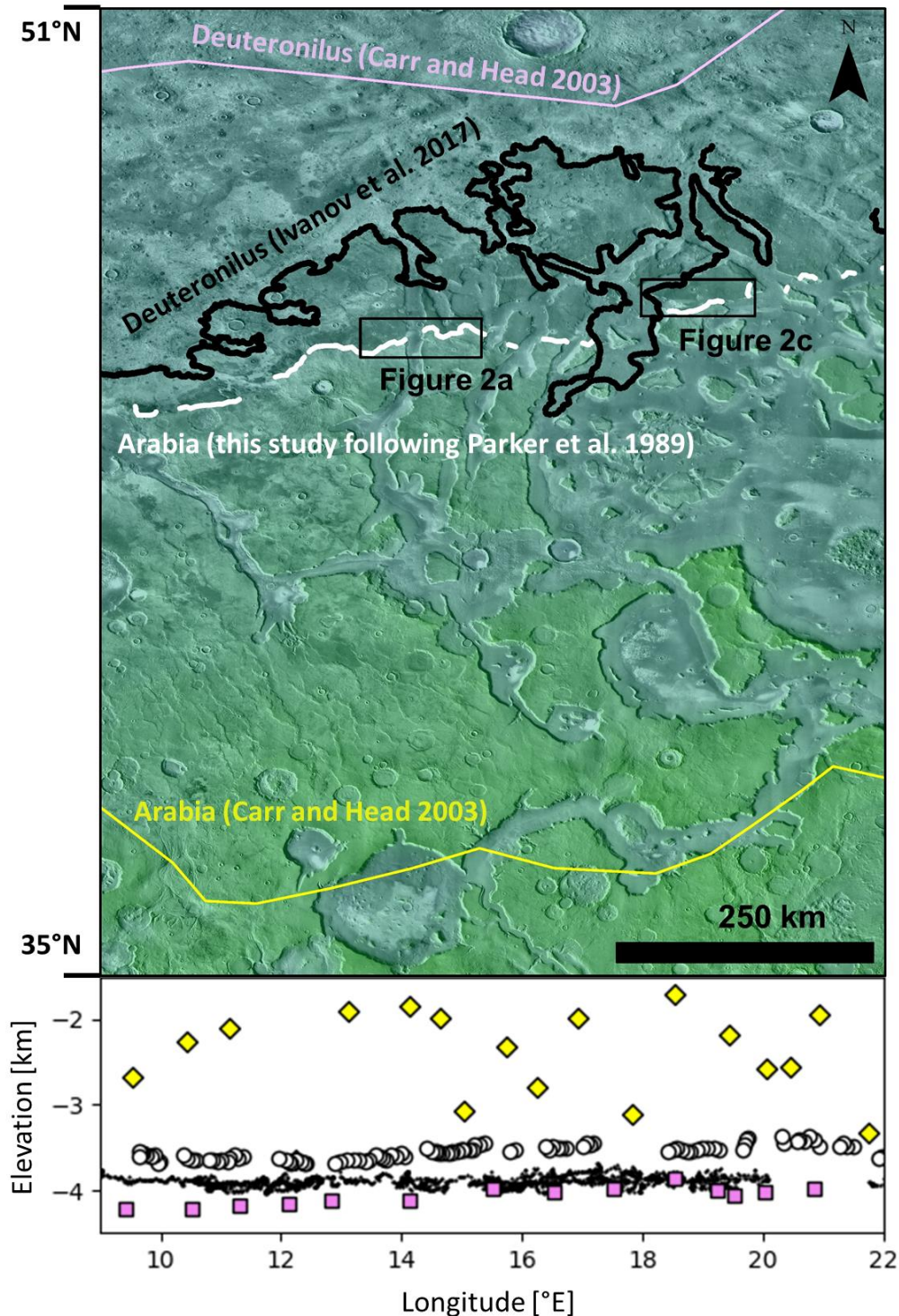


Figure 3: Lateral and topographic variations between different versions of the putative shorelines in Deuteronilus Mensae. *Top*) MOLA colorized elevation over THEMIS-IR daytime mosaic showing the shapefiles of the Arabia (yellow lines) and Deuteronilus (purple lines) from Carr and Head (2003) along with the Deuteronilus Level from Ivanov et al. (2017) (black lines) and our mapped version of the Arabia Level (white lines) based on the criteria set out in Parker et al. (1989). Black squares indicate areas in Figure 2. *Bottom*) Elevation data corresponding to the levels in the upper panel where the color of each symbol (yellow diamonds, white circles, black dots, and purple squares) matches the colors and delineated shapefiles in the upper panel.

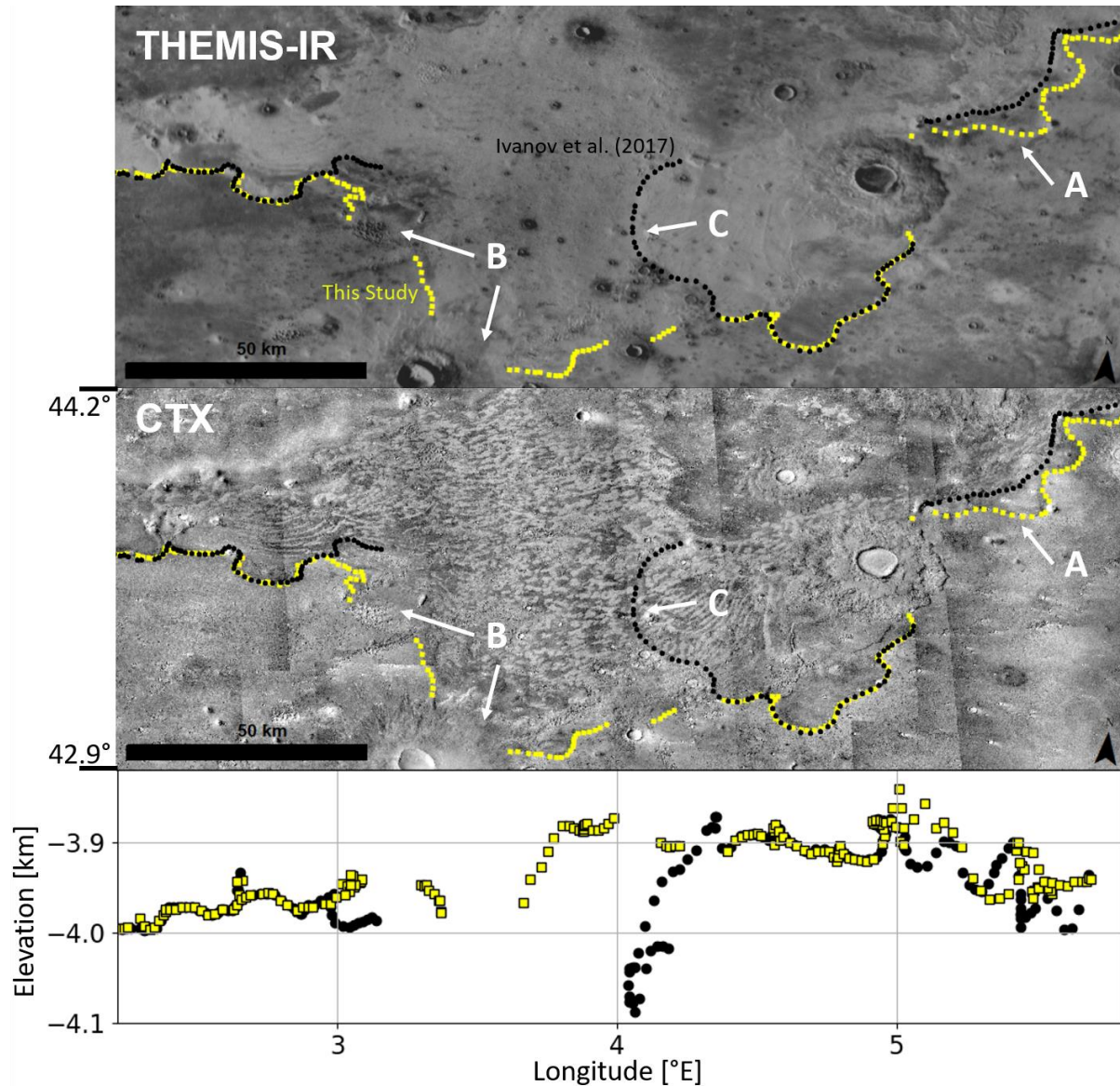


Figure 4: Offsets within the Deuteronilus Level remapping. THEMIS-IR daytime mosaic (*top*) showing Ivanov et al. (2017)'s remapped Deuteronilus Level following the southern boundary of the VBF (black dots) along with our remapped version (yellow squares) using both CTX (*middle*) and THEMIS-IR. *Bottom*: Corresponding elevation data for each of the mapped levels. A corresponds to underlying lobate flows that were incorrectly mapped. B corresponds to segments that were too subtle to be identified with the THEMIS mosaic. C corresponds to an internal contact within the VBF unit.

217

218

219

220

221

222

223

224

subtle at THEMIS resolutions. Even with CTX, crater ejecta and other surface processes leave our mapped contact discontinuous in some places; and C) erroneously mapped segments that represent intra-unit contacts. While commonly defined as a single unit, the VBF has a range of textural and tonal units throughout (Tanaka et al., 2003; Tanaka et al., 2005). For example, in THEMIS-IR mosaics, Segment C appears to follow the boundary between two distinct light-toned units, but in CTX imagery it becomes apparent that this contact separates two variant units of the thumbprint terrain.

225

226

Our remapping over a stretch of ~250 km leads to small adjustments in the elevation and location of the mapped levels. Between our remapping and that of Ivanov et al. (2017), the mean

227 elevation differed by 25 m, total range by 60 m, and interdecile range by 15 m. Locally, the
228 largest offset is caused by the intra-VBF contact mapping which created a 215 m deviation.
229 Compared with the observed differences seen in the Arabia Level, these are inconsequential, but
230 could compound over the global level.

231 3.2 Global Shoreline Locations

232 Our meta-analysis of the published maps for the Arabia and Deuteronilus Levels found
233 that while they overall follow the same general path, there are noticeable deviations between
234 them. Despite citing data obtained from the same base maps (Parker et al., 1993; Parker et al.,
235 1989), there are multiple instances of lateral deviations >500 km from these base maps. For
236 example the Ormö et al. (2004) Arabia Level largely follows the Parker et al. (1993) figure
237 (despite the improved Clifford and Parker (2001) map) with three major exceptions: a large
238 northward deviation of 350-1,400 km around Alba Mons, an ~700 km eastward offset in north
239 Isidis Planitia, and following the Olympus Mons aureole rather than the shield. Similar large
240 shifts are found elsewhere among the other maps (Figure 1a).

241 These discrepancies between levels appear to be the result of multiple factors including
242 digitization error, generalizing placement, combining data from multiple maps, and redrawing
243 sections based on new interpretations. The availability of MOLA topography also appears to
244 have led to a considerable reinterpretation of previously mapped levels, which were originally
245 mapped based on low-resolution geomorphological or albedo features.

246 Our first-order estimation of the maximum spatial variance of these offsets between all
247 the Arabia Level shapefiles finds that the different versions vary in latitudinal distance by an
248 average of 560 km globally. However, four sections have extreme variations of >1,000 km where
249 our methodology appears to grossly misrepresent the true lateral offset. These deviations along
250 the Olympus Mons aureole (-128°E to -150°E), western Chryse Planitia (-48°E to -57°E), and
251 western Isidis Planitia (77°E to 89°E) are due to the limitations of the near-longitudinally
252 tracking of the levels regionally, while the diversion along Amenthes Planum (99°E to 114°E)
253 neglects the recessed geometry of the planum (Figure 1d). A fifth section around Alba Mons also
254 exceeds 1,000 km, but this is a true representation of the plainsward redrawing of the level from
255 the base maps. If we exclude the four outlier sections, the mean deviation of the Arabia Level is
256 360 km with a maximum 1,350 km lateral offset which shows the poorly known location of the
257 Arabia Level.

258 We do not include global lateral offsets of the Deuteronilus Level, as we take the detailed
259 mapping shapefile of Ivanov et al. (2017) as the location of the level. This is because the
260 Deuteronilus Level is largely defined by a mappable contact (the VBF) unlike the Arabia Level,
261 which additionally has had no such published detailed remapping based on updated higher-
262 resolution data. However, Figure 1a still shows a high-degree of uncertainty in the location of the
263 Deuteronilus Level in mapping before Ivanov et al. (2017). Additionally, our results in Section
264 3.1 show that this mapping is still limited by the resolution and albedo variation of subunits, and
265 is incomplete in places.

266 The large spatial variance between the different versions of each level contributes to a
267 high degree of uncertainty with the elevation data for each level. Given no standard definition of
268 where the Arabia Level is located, not only is there a large topographic range to the level, but
269 also a large range in the mean elevation across different mappings. The mean elevation between

270 the different Arabia Level versions varies by ~1.7 km: Webb (2004) data have a mean elevation
 271 as low as -3.84 km and Carr and Head (2003) data have it as high as -2.12 km. The interdecile
 272 range within each of the global Arabia Level versions varies from 1.05 km (Fairén et al., 2003)
 273 to 3.84 km (Parker et al., 1993). This large variation echoes the conclusions of other studies that
 274 found a potential ~2 km topographic offset due to the misidentification of the Arabia Level near
 275 Apollinaris Patera (Parker & Calef, 2012). A table of statistics for each of our digitized versions
 276 and author-supplied shapefiles of the mapped levels is presented in Table 1.

277 Locations of deltas have also been invoked to validate the levels as paleoshorelines, so
 278 we also compare their topographic and lateral locations with both Levels (Figure 1). Di Achille
 279 and Hynek (2010) proposed a list of 17 open-basin deltas which equated to an ocean level at -
 280 2.54 ± 0.18 km. These deltas generally fall along the southern-bounds of the different Arabia
 281 Level versions but 6 do not fall within the ranges. Topographically, they all generally fall within
 282 the mapped levels, but given the 8.66 km spread of elevation range, this is unsurprising.
 283 Additionally, detailed higher-resolution studies have found that many of these open deltas fall
 284 within localized enclosed basins and have been reinterpreted to be from paleolakes rather than a
 285 northern ocean or sea (Rivera-Hernandez & Palucis, 2019).

286

287 **Table 1: Elevation data, in kilometers, and statistics of the digitized Arabia and Deuteronilus Levels.**
 288 Webb (2004) and this study are limited regional remapping. Ivanov et al. (2017) and Perron et al. (2007)
 289 are the original shapefiles provided by the authors, rather than digitized levels.

	Citation	Mean	Standard Deviation	Max	Min	Range	10 th Percentile	90 th Percentile	Interdecile Range
Arabia	Parker et al. 1989	-2.78	1.11	2.23	-5.01	7.24	-3.82	-1.39	2.43
	Parker et al. 1993	-2.13	1.47	3.19	-5.47	8.67	-3.81	0.04	3.84
	Clifford and Parker 2001	-2.35	1.33	2.43	-4.56	6.99	-3.86	-0.46	3.39
	Carr and Head 2003	-2.12	1.29	1.18	-4.67	5.85	-3.75	-0.54	3.21
	Fairén et al. 2003	-3.40	0.49	-1.71	-4.73	3.02	-3.84	-2.79	1.05
	Ormo et al. 2004	-2.42	0.95	1.77	-5.13	6.90	-3.47	-1.10	2.37
	Webb 2004	-3.84	0.04	-3.65	-3.98	0.34	-3.86	-3.81	0.05
	Perron et al. 2007	-2.37	1.20	0.44	-4.67	5.12	-3.77	-0.57	3.20
	This Study	-3.56	0.08	-3.33	-3.69	0.36	-3.66	-3.46	0.19
Deuteronilus	Parker et al. 1989	-4.33	0.60	-2.72	-5.21	2.49	-4.98	-3.48	1.50
	Parker et al. 1993	-3.77	0.47	-2.13	-5.07	2.94	-4.18	-3.33	0.85
	Clifford and Parker 2001	-3.96	0.36	-3.16	-5.22	2.06	-4.58	-3.59	0.99
	Carr and Head 2003	-3.81	0.26	-2.95	-5.02	2.07	-4.14	-3.47	0.66
	Ormo et al. 2004	-3.76	0.19	-1.90	-4.93	3.03	-3.98	-3.58	0.40
	Ivanov et al. 2017	-3.76	0.21	-3.17	-4.19	1.02	-4.02	-3.48	0.54

290 4 Conclusions

291 The Arabia Level, as presented through maps in the published literature, deviates
 292 significantly from the location of the proposed definition described originally by Parker et al.
 293 (1989). In particular, our investigation of the putative shorelines within the Deuteronilus Mensae
 294 region found that the Arabia Level varied by up to 500 km laterally from traditionally used
 295 shapefiles (Carr & Head, 2003), which equates to a regional topographic difference greater than

296 1.1 km. This substantial offset is the result of the generalization of digitized maps and error
297 propagation that have continued to this day due to the lack of publicly available and standardized
298 shapefiles for each of the levels.

299 Furthermore, our global analysis of different maps for the Arabia Level finds that this
300 lateral offset extends globally up to ~1,300 km and with an average offset of 360 km between
301 versions. This large lateral displacement creates a high variance in the elevation of the levels
302 with mean elevations ranging from -2.1 km to -3.8 km and ranges within individual levels up to
303 8.7 km. Unlike the Deuteronilus Level, which is largely defined by the southern boundary of the
304 VBF, the Arabia Level has no rigorous definition and often exhibits multiple different
305 morphologies making it much more difficult to map in its entirety, further contributing to the
306 wide variance observed.

307 Historically, the maps used for both discontinuous segments of the Arabia and
308 Deuteronilus Levels have been generalized into smoothed and extrapolated very loose fits (e.g.
309 Carr and Head (2003) in Figure 1), which is insufficient for understanding the true topographic
310 disparity. The Arabia Level is particularly vulnerable to having incorrect elevation because it
311 straddles the topographic dichotomy. Combined with a history of using various versions of
312 datamined maps based on low-resolution Viking imagery, the location of the Arabia Level has
313 much greater uncertainty than the Deuteronilus Level.

314 The offset between different versions of the Arabia Level is particularly important when
315 trying to assess why the level does not meet an expected equipotential surface. Geophysical
316 deformation models have attempted to use these data to explain how long-wavelength processes
317 can create the vast spread in observed elevations of the levels. However, for the Arabia Level,
318 these models have neglected major mapped portions of the level (e.g., Chan et al., 2018; Citron
319 et al., 2018; Perron et al., 2007). We have also shown that not only is there wide uncertainty in
320 its mapped location, there is a lack of a standardized definition, and large variation in
321 topographic ranges both between and within mapped levels. Thus, caution is warranted when
322 using these data and deriving sweeping conclusions about the history of Mars. The wide variance
323 with the mean elevation and intra-level range can considerably shift the narrative of the timing,
324 extent, and water inventory of such hypothesized oceans.

325 The interpretation of the margins of the lowland boundaries remains controversial, which
326 is compounded by the uncertainties in mapping laid bare in this paper. The Deuteronilus Level
327 has been more rigorously studied, has a narrower topographic range and may be consistent with
328 deposits from an ice- and debris-covered ocean (Carr & Head, 2019; Ivanov et al., 2017;
329 Kreslavsky & Head, 2002; Parker et al., 2010). However, this contact may also be the result of
330 more other processes that are plausible for Mars, such as volcanic, glacial, or subaerial
331 catastrophic flood deposits (Jöns, 1985; Salvatore & Christensen, 2014; Tanaka et al., 2001;
332 Tanaka et al., 2003). The wide topographic and spatial range of the Arabia Level does not
333 strongly support an ocean hypothesis and may simply be the result of the degradation of the
334 highlands or exposure of different lithological units along the topographic dichotomy (Sholes et
335 al., 2019; Tanaka, 1997).

336 Overall, the wide displacement between maps of the hypothesized shorelines shows how
337 inaccurate and inconsistent the global mapping of paleoshorelines has been. The Arabia Level
338 maps are particularly poor and require an updated high-resolution global remapping effort fully
339 detailing the global geologic and geomorphic expressions. While these results do not preclude

340 the existence of oceans, more compelling evidence is required to support an interpretation of
341 oceans.

342 **Acknowledgments**

343 We thank Mikhail Ivanov and Taylor Perron for sharing shapefiles of their mapped levels. S.F.S.
344 and D.C.C. were partially supported by NASA Astrobiology Institute grant NNA13AA93A.
345 Z.I.D. was partially supported by Science and Technology Facilities Council grant STFC-
346 1967420.

347 **Supplemental Data**

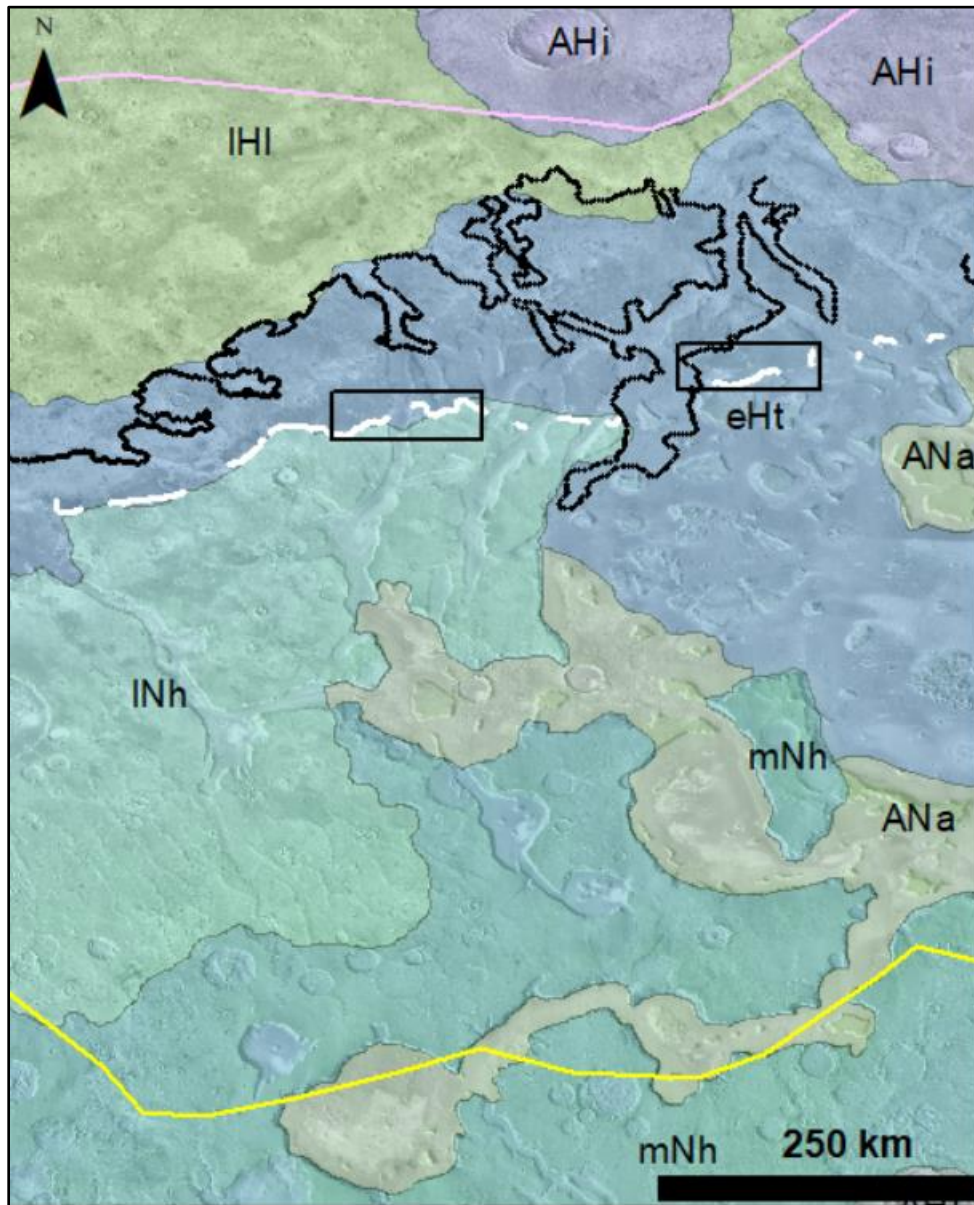
348 We provide our mapped and digitized levels as supplemental data which is also archived at doi:
349 10.5281/zenodo.3743911.

350

351

352 **Appendix A**

353



354

355

356 **Figure A1: Geological units overlain on Figure 3 (MOLA colored elevation over THEMIS-IR daytime mosaic).**

357 Our mapped Arabia Level (white lines) roughly follows the contact between the early Hesperian transitional (eHt)

358 unit and the late Noachian highlands (INh) unit. The Deuteronilus Level roughly follows the contact between the

359 eHt and late Hesperian lowlands (IHI) units. mNh: middle Noachian highlands unit, ANa: Amazonian and Noachian

360 apron unit, AHi: Amazonian and Hesperian impact unit (Tanaka et al., 2014). Colored lines indicate the shapefiles

361 of the Arabia (yellow lines) and Deuteronilus (purple lines) from Carr and Head (2003) along with the Deuteronilus

362 Level from Ivanov et al. (2017) (black lines) and our mapped version of the Arabia Level (white lines) based on the

363 criteria set out in Parker et al. (1989).

364

364

365 **References**

- 366
367 Aharonson, O., Zuber, M. T., & Rothman, D. H. (2001). Statistics of Mars' topography from the Mars Orbiter Laser
368 Altimeter: Slopes, correlations, and physical models. *Journal of Geophysical Research: Planets*, 106(E10),
369 23723-23735. doi:10.1029/2000JE001403
- 370 Baker, D. M., & Head, J. W. (2015). Extensive Middle Amazonian mantling of debris aprons and plains in
371 Deuteronilus Mensae, Mars: Implications for the record of mid-latitude glaciation. *Icarus*, 260, 269-288.
372 doi:10.1016/j.icarus.2015.06.036
- 373 Carr, M. H., & Head, J. W. (2003). Oceans on Mars: An assessment of the observational evidence and possible fate.
374 *Journal of Geophysical Research: Planets*, 108(E5), 5042. doi:10.1029/2002JE001963
- 375 Carr, M. H., & Head, J. W. (2019). Mars: Formation and fate of a frozen Hesperian ocean. *Icarus*, 319, 433-443.
376 doi:10.1016/j.icarus.2018.08.021
- 377 Chan, N. H., Perron, J. T., Mitrovica, J. X., & Gomez, N. A. (2018). New Evidence of an Ancient Martian Ocean
378 from the Global Distribution of Valley Networks. *Journal of Geophysical Research: Planets*, 123(8), 2138-
379 2150. doi:10.1029/2018JE005536
- 380 Christensen, P. R., Jakosky, B. M., Kieffer, H. H., Malin, M. C., McSween, H. Y., Jr., Nealon, K., et al. (2004).
381 The Thermal Emission Imaging System (THEMIS) for the Mars 2001 Odyssey Mission. *Space Science*
382 *Reviews*, 110(1-2), 85-130. doi:10.1023/B:SPAC.0000021008.16305.94
- 383 Citron, R. I., Manga, M., & Hemingway, D. J. (2018). Timing of oceans on Mars from shoreline deformation.
384 *Nature*, 555(7698), 643-646. doi:10.1038/nature26144
- 385 Clifford, S. M., & Parker, T. J. (2001). The Evolution of the Martian Hydrosphere: Implications for the Fate of a
386 Primordial Ocean and the Current State of the Northern Plains. *Icarus*, 154(1), 40-79.
387 doi:10.1006/icar.2001.6671
- 388 Di Achille, G., & Hynek, B. M. (2010). Ancient ocean on Mars supported by global distribution of deltas and
389 valleys. *Nature Geoscience*, 3(7), 459-463. doi:10.1038/ngeo891
- 390 Edgett, K. S., & Parker, T. J. (1997). Water on early Mars: Possible subaqueous sedimentary deposits covering
391 ancient cratered terrain in western Arabia and Sinus Meridiani. *Geophysical Research Letters*, 24(22),
392 2897-2900. doi:10.1029/97GL02840
- 393 Fairen, A. G., Dohm, J. M., Baker, V. R., de Pablo, M. A., Ruiz, J., Ferris, J. C., & Anderson, R. C. (2003). Episodic
394 flood inundations of the northern plains of Mars. *Icarus*, 165(1), 53-67. doi:10.1016/S0019-
395 1035(03)00144-1
- 396 Ferguson, R. L., Hare, T. M., & Laura, J. (2018). HRSC and MOLA Blended Digital Elevation Model at 200m v2.
397 *USGS Astrogeology Science Center*.
- 398 Ghatan, G. J., & Zimbelman, J. R. (2006). Paucity of candidate coastal constructional landforms along proposed
399 shorelines on Mars: Implications for a northern lowlands-filling ocean. *Icarus*, 185(1), 171-196.
400 doi:10.1016/j.icarus.2006.06.007
- 401 Head, J. W., Hiesinger, H., Ivanov, M. A., Kreslavsky, M. A., Pratt, S., & Thomson, B. J. (1999). Possible ancient
402 oceans on Mars: evidence from Mars Orbiter Laser Altimeter data. *Science*, 286(5447), 2134-2137.
403 doi:10.1126/science.286.5447.2134
- 404 Head, J. W., Kreslavsky, M., Hiesinger, H., Ivanov, M., Pratt, S., Seibert, N., et al. (1998). Oceans in the past history
405 of Mars: Tests for their presence using Mars Orbiter Laser Altimeter (MOLA) data. *Geophysical Research*
406 *Letters*, 25(24), 4401-4404. doi:10.1029/1998GL900116
- 407 Ivanov, M. A., Erkeling, G., Hiesinger, H., Bernhardt, H., & Reiss, D. (2017). Topography of the Deuteronilus
408 contact on Mars: Evidence for an ancient water/mud ocean and long-wavelength topographic
409 readjustments. *Planetary and Space Science*, 144, 49-70. doi:10.1016/j.pss.2017.05.012
- 410 Jaumann, R., Neukum, G., Behnke, T., Duxbury, T. C., Eichtenopf, K., Flohrer, J., et al. (2007). The high-resolution
411 stereo camera (HRSC) experiment on Mars Express: Instrument aspects and experiment conduct from
412 interplanetary cruise through the nominal mission. *Planetary and Space Science*, 55(7-8), 928-952.
413 doi:10.1016/j.pss.2006.12.003
- 414 Jöns, H.-P. (1985). *Late sedimentation and late sediments in the northern lowlands on Mars*. Paper presented at the
415 16th Lunar Planetary Science Conference, 414-415.
- 416 Kreslavsky, M. A., & Head, J. W. (2002). Fate of outflow channel effluents in the northern lowlands of Mars: The
417 Vastitas Borealis Formation as a sublimation residue from frozen ponded bodies of water. *Journal of*
418 *Geophysical Research*, 107, 5121. doi:10.1029/2001JE001831

- 419 Leverington, D., & Ghent, R. (2004). Differential subsidence and rebound in response to changes in water loading
 420 on Mars: Possible effects on the geometry of ancient shorelines. *Journal of Geophysical Research: Planets*,
 421 109(E1). doi:10.1029/2003JE002141
- 422 Malin, M. C., Bell, J. F., Cantor, B. A., Caplinger, M. A., Calvin, W. M., Clancy, R. T., et al. (2007). Context
 423 camera investigation on board the Mars Reconnaissance Orbiter. *Journal of Geophysical Research:*
 424 *Planets*, 112(E5), E05S04. doi:10.1029/2006JE002808
- 425 Malin, M. C., & Edgett, K. S. (1999). Oceans or seas in the Martian northern lowlands: High resolution imaging
 426 tests of proposed coastlines. *Geophysical Research Letters*, 26(19), 3049-3052.
 427 doi:10.1029/1999GL002342
- 428 Malin, M. C., & Edgett, K. S. (2001). Mars Global Surveyor Mars Orbiter Camera: Interplanetary cruise through
 429 primary mission. *Journal of Geophysical Research: Planets*, 106(E10), 23429-23570.
 430 doi:10.1029/2000JE001455
- 431 Mangold, N., & Howard, A. D. (2013). Outflow channels with deltaic deposits in Ismenius Lacus, Mars. *Icarus*,
 432 226(1), 385-401. doi:10.1016/j.icarus.2013.05.040
- 433 McEwen, A. S., Eliason, E. M., Bergstrom, J. W., Bridges, N. T., Hansen, C. J., Delamere, W. A., et al. (2007).
 434 Mars Reconnaissance Orbiter's High Resolution Imaging Science Experiment (HiRISE). *Journal of*
 435 *Geophysical Research: Planets*, 112(E5), E05S02. doi:10.1029/2005JE002605
- 436 Morgan, G. A., Head III, J. W., & Marchant, D. R. (2009). Lineated valley fill (LVF) and lobate debris aprons
 437 (LDA) in the Deuteronilus Mensae northern dichotomy boundary region, Mars: Constraints on the extent,
 438 age and episodicity of Amazonian glacial events. *Icarus*, 202(1), 22-38. doi:10.1016/j.icarus.2009.02.017
- 439 Ormö, J., Dohm, J. M., Ferris, J. C., Lepinette, A., & Fairén, A. G. (2004). Marine-target craters on Mars? An
 440 assessment study. *Meteoritics & Planetary Science*, 39(2), 333-346. doi:10.1111/j.1945-
 441 5100.2004.tb00344.x
- 442 Parker, T. J., & Calef, F. J. (2012). *Digital Global Map of Potential Ocean Paleoshorelines on Mars*. Paper
 443 presented at the Third Conference on Early Mars, 7085.
- 444 Parker, T. J., Gorsline, D. S., Saunders, R. S., Pieri, D. C., & Schneeberger, D. M. (1993). Coastal geomorphology
 445 of the Martian northern plains. *Journal of Geophysical Research: Planets*, 98(E6), 11061-11078.
 446 doi:10.1029/93JE00618
- 447 Parker, T. J., Grant, J. A., & Franklin, B. J. (2010). The northern plains: A Martian oceanic basin? In N. A. Cabrol &
 448 E. A. Grin (Eds.), *Lakes on Mars* (pp. 249-273). Boston: Elsevier.
- 449 Parker, T. J., Saunders, S. R., & Schneeberger, D. M. (1989). Transitional morphology in West Deuteronilus
 450 Mensae, Mars: Implications for modification of the lowland/upland boundary. *Icarus*, 82(1), 111-145.
 451 doi:10.1016/0019-1035(89)90027-4
- 452 Perron, J. T., Mitrovica, J. X., Manga, M., Matsuyama, I., & Richards, M. A. (2007). Evidence for an ancient
 453 martian ocean in the topography of deformed shorelines. *Nature*, 447(7146), 840-843.
 454 doi:10.1038/nature05873
- 455 Rivera-Hernandez, F., & Palucis, M. C. (2019). Do deltas along the crustal dichotomy boundary of Mars in the Gale
 456 crater region record a northern ocean? *Geophysical Research Letters*. doi:10.1029/2019GL083046
- 457 Roberts, J. H., & Zhong, S. (2004). Plume-induced topography and geoid anomalies and their implications for the
 458 Tharsis rise on Mars. *Journal of Geophysical Research: Planets*, 109(E3). doi:10.1029/2003JE002226
- 459 Ruiz, J., Fairen, A. G., Dohm, J. M., & Tejero, R. (2004). Thermal isostasy and deformation of possible
 460 paleoshorelines on Mars. *Planetary and Space Science*, 52(14), 1297-1301. doi:10.1016/j.pss.2004.06.003
- 461 Salvatore, M. R., & Christensen, P. (2014). On the origin of the vastitas borealis formation in chryse and acidalia
 462 planitiae, mars. *Journal of Geophysical Research: Planets*, 119(12), 2437-2456.
 463 doi:10.1002/2014JE004682
- 464 Sholes, S. F. (2019). *Geomorphic and Atmospheric Investigations on the Habitability of Past and Present Mars*.
 465 (Doctoral Degree), University of Washington, Seattle, WA.
- 466 Sholes, S. F., Montgomery, D. R., & Catling, D. C. (2019). Quantitative High-Resolution Reexamination of a
 467 Hypothesized Ocean Shoreline in Cydonia Mensae on Mars. *Journal of Geophysical Research: Planets*,
 468 124(2), 316-336. doi:10.1029/2018JE005837
- 469 Smith, D. E., Zuber, M., Frey, H., Garvin, J., Head, J., Muhleman, D., et al. (1998). Topography of the northern
 470 hemisphere of Mars from the Mars Orbiter Laser Altimeter. *Science*, 279(5357), 1686-1692.
 471 doi:10.1126/science.279.5357.1686
- 472 Smith, D. E., Zuber, M. T., Frey, H. V., Garvin, J. B., Head, J. W., Muhleman, D. O., et al. (2001). Mars Orbiter
 473 Laser Altimeter: Experiment summary after the first year of global mapping of Mars. *Journal of*
 474 *Geophysical Research: Planets*, 106(E10), 23689-23722. doi:10.1029/2000JE001364

- 475 Tanaka, K. L. (1997). Sedimentary history and mass flow structures of Chryse and Acidalia Planitiae, Mars. *Journal*
476 *of Geophysical Research: Planets*, 102(E2), 4131-4149. doi:10.1029/96JE02862
- 477 Tanaka, K. L., Banerdt, W. B., Kargel, J. S., & Hoffman, N. (2001). Huge, CO₂-charged debris-flow deposit and
478 tectonic sagging in the northern plains of Mars. *Geology*, 29(5), 427-430. doi:10.1130/0091-
479 7613(2001)029<0427:HCCDFD>2.0.CO;2
- 480 Tanaka, K. L., Robbins, S. J., Fortezzo, C. M., Skinner, J. A., & Hare, T. M. (2014). The digital global geologic map
481 of Mars: Chronostratigraphic ages, topographic and crater morphologic characteristics, and updated
482 resurfacing history. *Planetary and Space Science*, 95, 11-24. doi:10.1016/j.pss.2013.03.006
- 483 Tanaka, K. L., Skinner, J. A., Hare, T. M., Joyal, T., & Wenker, A. (2003). Resurfacing history of the northern
484 plains of Mars based on geologic mapping of Mars Global Surveyor data. *Journal of Geophysical*
485 *Research: Planets*, 108(E4). doi:10.1029/2002JE001908
- 486 Tanaka, K. L., Skinner, J. A., Jr., & Hare, T. M. (Cartographer). (2005). Geologic map of the northern plains of
487 Mars
- 488 Webb, V. E. (2004). Putative shorelines in northern Arabia Terra, Mars. *Journal of Geophysical Research: Planets*,
489 109(E09010). doi:10.1029/2003JE002205
- 490 Zuber, M. T. (2018). Oceans on Mars formed early. *Nature*, 555, 590-591. doi:10.1038/d41586-018-03415-x
491